Z. Phys. B – Condensed Matter 86, 49–52 (1992)

Condensed
Zeitschrift für Physik B Matter

Hartree-Fock theory of spiral magnetic order in the 2-*d* Hubbard model

M. Dzierzawa

Institut für Theorie der Kondensierten Materie, Universität Karlsruhe, Postfach 6980, W-7500 Karlsruhe 1, Federal Republic of Germany

Received August 2, 1991

The magnetic order in the 2-*d* Hubbard model is investigated within Hartree-Fock theory. For the class of states with uniform particle density and spiral arrangement of spins the phase diagram is obtained by minimizing the free energy. At zero temperature and large Hubbard interaction U there is a continuous transition from the antiferromagnetic solution at half filling over a spiral state of increasing wavelength along the diagonal of the lattice to the ferromagnetic state at doping $\delta_c \approx 2t/U$. At finite temperature T, the antiferromagnetic state remains stable for doping smaller than $\delta_{AF} \approx 2T/U$. For

The simplest theoretical description is provided by the Hartree-Fock approximation, which allows, at least numerically, for a detailed analysis of the solutions. Investigations along this line have been carried through by several authors [5–8]. A more involved approach is the slave boson method, where electronic correlations are taken into account in a systematic way, but even the mean field approximation of the slave boson theory for systems with broken symmetry requires considerable numerical efforts [9].

In this paper numerical solutions of the Hartree-Fock

where $\hat{\boldsymbol{\sigma}}_i = \sum_{s,s'} \hat{c}_{is}^{+} \boldsymbol{\sigma}_{ss'} \hat{c}_{is'}$ and $\boldsymbol{\sigma}$ are the Pauli matrices. The minimization of the free energy with respect to the fields ρ_i and $\mathbf{m}_i$ yields the self-consistency equations

$$\rho_i = \langle \hat{n}_i \rangle, \quad \mathbf{m}_i = \langle \hat{\boldsymbol{\sigma}}_i \rangle. \tag{2.3}$$

Here we restrict to solutions with uniform density $\rho_i \equiv \rho$ and spiral arrangement of the magnetic moments in the x-y-plane

$$\mathbf{m}_i = m(\cos \mathbf{Q}\mathbf{R}_i, \sin \mathbf{Q}\mathbf{R}_i, 0). \tag{2.4}$$

This subclass of Hartree-Fock Hamiltonians can be diagonalized by introducing new fermion operators in k-space

$$\begin{aligned} \hat{d}_{k1}^{+} &= u_k \hat{c}_{k\uparrow}^{+} + v_k \hat{c}_{k+Q\downarrow}^{+} \\ \hat{d}_{k2}^{+} &= -v_k \hat{c}_{k\uparrow}^{+} + u_k \hat{c}_{k+Q\downarrow}^{+} \end{aligned} \tag{2.5}$$

which form two bands with quasi-particle dispersion

$$E_k^{(1,2)} = \varepsilon_{k+} \mp \sqrt{\varepsilon_{k-}^2 + \Delta^2} \tag{2.6}$$

where $\varepsilon_{k\pm} = (\varepsilon_k \pm \varepsilon_{k+Q})/2$ with the free particle dispersion $\varepsilon_k = -2t(\cos k_x + \cos k_y)$ and the gap parameter $\Delta = mU/2$.

The free energy (per site) of the Hartree-Fock spiral state is given by

$$F = -T \frac{1}{N} \sum_{k,n} \ln(1 + \exp -(E_k^{(n)} - \mu)/T) + \mu\rho + \frac{U}{4}(\rho^2 + m^2) \tag{2.7}$$

where the chemical potential μ is chosen such that

$$\rho = \frac{1}{N} \sum_{k,n} f(E_k^{(n)} - \mu). \tag{2.8}$$

Minimization of F with respect to Δ and $\mathbf{Q}$ yields the following set of equations

$$\frac{1}{N} \sum_{k,n} (-)^{n+1} \frac{f(E_k^{(n)} - \mu)}{\sqrt{\varepsilon_{k-}^2 + \Delta^2}} = \frac{2}{U} \tag{2.9}$$

and

$$\tan(Q_\alpha/2) \sum_{k,n} f(E_k^{(n)} - \mu) \cos k_\alpha = \sum_{k,n} (-)^n f(E_k^{(n)} - \mu) \frac{\varepsilon_{k-} \sin k_\alpha}{\sqrt{\varepsilon_{k-}^2 + \Delta^2}} \tag{2.10}$$

which generally can only be solved numerically. The calculations presented here are done for lattices up to 128×128 sites to make sure that finite size effects are under control.

3. Phase diagram at zero temperature

The results of the numerical solution of the Hartree-Fock equations at $T = 0$ are summarized in the $\delta - U$ phase diagram displayed in Fig. 1. The antiferromagnetic phase is strictly confined to the line $\delta = 0$. The different spiral phases appearing with doping are characterized by their wave-vector $\mathbf{Q}$. Close to half filling $\mathbf{Q}$ is of the form (Q, Q) with $0 < Q < \pi$, which corresponds to a spiral along the diagonal of the lattice. The wave-vector $\mathbf{Q} = (Q, \pi)$ appearing at somewhat larger doping for small and intermediate values of U describes a spiral with wavenumber Q in x-direction and antiferromagnetic order in y-direction. The appearance of the (Q, π) rather than the (Q, Q) spiral in the small U region is due to the fact, that upon doping the maximum of the susceptibility $\chi(\mathbf{q})$ in the paramagnetic state is moving from (π, π) to $(0, \pi)$ and not along the diagonal of the Brillouin zone. A special case of the (Q, π) spiral is the state with $\mathbf{Q} = (0, \pi)$, where the system is ferromagnetic in one and antiferromagnetic in the other direction.

The most interesting part of the phase diagram is the region close to half filling, where for large U the transition from antiferro- to ferromagnetism occurs. Here the two quasi-particle bands are well separated and the lower band is nearly completely filled.

To get an idea about the dispersion of the (Q, Q)-spiral close to the top of the lower band it is convenient to rewrite (2.6) using

$$\begin{aligned} \varepsilon_{k+} &= -2t \cos(Q/2)(\cos(k_x + Q/2) + \cos(k_y + Q/2)) \\ \varepsilon_{k-} &= -2t \sin(Q/2)(\sin(k_x + Q/2) + \sin(k_y + Q/2)). \end{aligned} \tag{3.1}$$

While for the antiferromagnet ($Q = \pi$) the states with $|k_x \pm k_y| = \pi$ are degenerate and highest in energy, for $Q < \pi$ there is a single maximum at $\mathbf{k}_0 = (\pi - Q/2, \pi - Q/2)$. Close to $\mathbf{k}_0$ the dispersion can be approximated by

$$E_k^{(1)} = E_0 - (t_\perp k_\perp^2 + t_{\parallel} k_{\parallel}^2) \tag{3.2}$$

where

$$\begin{aligned} t_{\parallel} &= t \cos(Q/2) \\ t_\perp &= t \cos(Q/2) + 4(t^2/\Delta) \sin^2(Q/2) \end{aligned} \tag{3.3}$$

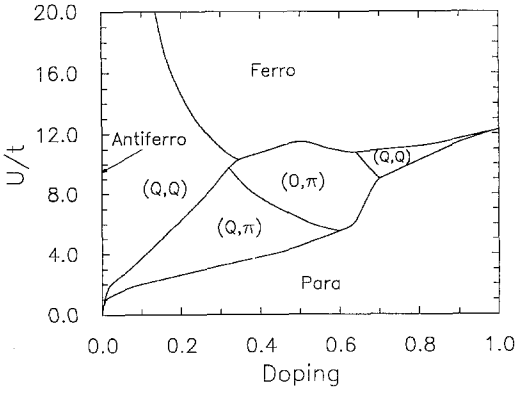

Fig. 1. $\delta - U$ phase diagram at $T = 0$. The spiral phases are denoted by the spiral wave-vector $\mathbf{Q}$. In the phases (Q, Q) and (Q, π) the wave-number Q varies between 0 and π

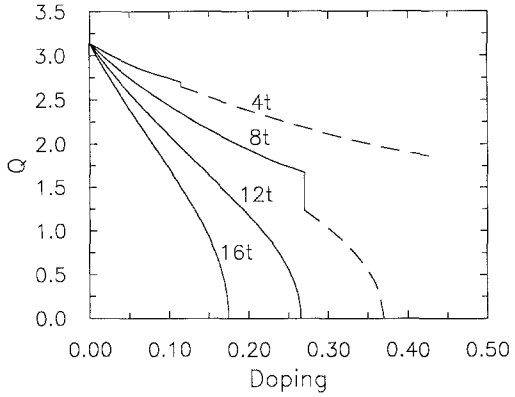

Fig. 2. Spiral wave-vector **Q** as function of doping δ for $U=4t$, $8t$, $12t$, $16t$ at $T=0$. Full curve: $\mathbf{Q}=(Q,Q)$, dashed curve: $\mathbf{Q}=(Q,\pi)$

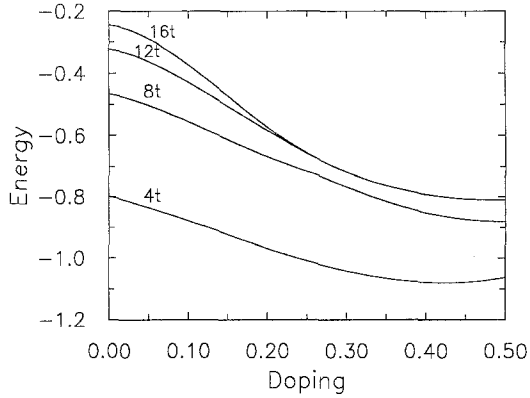

Fig. 3. Groundstate energy as function of doping for $U=4t$, $8t$, $12t$, $16t$

is the hopping parallel (perpendicular) to the line $k_x+k_y=\pi$. In lowest order in t/U equations (2.8–2.10) lead to

$$\Delta=U(1-\delta)/2$$

$$\cos(Q/2)=\frac{\Delta\delta}{t}\frac{1-(\pi/4)(\gamma+1/\gamma)\,\delta}{1-2\pi\gamma\delta^2} \tag{3.4}$$

with $\gamma=\sqrt{t_{\|}/t_{\perp}}$. Close to the transition to the ferromagnetic state $Q\to 0$ and $\gamma\to 1$, consequently

$$\cos(Q/2)=\frac{\Delta\delta}{t}\frac{1-(\pi/2)\,\delta}{1-2\pi\delta^2} \tag{3.5}$$

which implies, that at the transition Q vanishes like a square-root,

$$Q\sim(\delta_c-\delta)^{1/2} \qquad \text{with } \delta_c=2t/U+(1+\pi/2)(2t/U)^2.$$

Close to the antiferromagnetic phase ($Q\to\pi$) an expansion for small δ yields

$$\cos(Q/2)=(U/2t)\,\delta-(\pi/2)\,\delta^{3/2}. \tag{3.6}$$

For the (Q,π)-spiral the top of the lower band is along the line $k_x=\pi-Q/2$. In the limit $t/U\ll 1$ the x-component Q of the spiral vector is given by

$$\cos(Q/2)=\frac{\Delta}{t}\frac{2\sin\pi\delta}{2\pi(1-\delta)+\sin 2\pi\delta}. \tag{3.7}$$

It follows, that the transition to the $(0,\pi)$-spiral takes place at

$$U_c=t\frac{2\pi(1-\delta)+\sin 2\pi\delta}{(1-\delta)\sin\pi\delta} \tag{3.8}$$

e.g. for $\delta=0.5$ at $U_c=2\pi t$.

In Fig. 2 the x-component of the spiral wavevector **Q** is plotted as a function of doping δ for $U=4t$, $8t$, $12t$, $16t$. For $U=4t$ the transition from the (Q,Q) to the (Q,π) spiral (dashed curve) takes place at $\delta=0.12$ and for $U=8t$ at $\delta=0.27$. In both cases the x-component figure, jumps to π. For $U=4t$ the curve ends at $\delta=0.44$, where the transition to the paramagnetic state takes place, while for $U=8t$ the $(0,\pi)$-spiral is reached at $\delta=0.37$. For larger values of U the spiral wave-vector decreases continuously along the diagonal of the Brillouin zone from $\mathbf{Q}=(\pi,\pi)$ at $\delta=0$ to $\mathbf{Q}=(0,0)$ at $\delta=0.26(U=12t)$ and $\delta=0.18(U=16t)$.

In the same limit of large U and small doping one can use the above results to calculate the groundstate energy as a function of doping. Including quadratic terms in δ one finds for the (Q,Q)-spiral

$$E(\delta)=-4t^2/U-(4t^2/U)\,\delta-U\delta^2 \tag{3.9}$$

and for the (Q,π)-spiral

$$E(\delta)=-4t^2/U-(2t^2/U)\,\delta-(U/2)\,\delta^2 \tag{3.10}$$

which shows that the (Q,Q)-spiral is better in energy for large U. In Fig. 3 the groundstate energy is plotted as a function of δ for $U=4t$, $8t$, $12t$, $16t$. For large U and small doping the second derivative of the energy is negative, indicating that the system is unstable against phase separation. Comparison with the phase diagram (see Fig. 1) shows, that nearly the whole (Q,Q)-spiral is affected. It is an interesting question, into which kind of non-homogeneous phase the system would turn in this region if the Hartree-Fock solutions were not restricted to uniform spiral states.

4. Finite temperatures

The most interesting effect of finite temperatures is found close to half-filled band. Whereas in the case $T=0$ the antiferromagnetic state changes into the (Q,Q) spiral for arbitrary small doping, for $T>0$, there exists a finite range of doping, where the antiferromagnetic state remains stable. In order to determine the range of stability one has to calculate the second derivative of the free energy with respect to the spiral vector at $Q=\pi$

$$\frac{\partial^2 F}{\partial Q^2}\bigg| \quad =\frac{1}{4N}\sum\left(f'(E_k^{(1)}-\mu)\,\varepsilon_{k+}^2-f(E_k^{(1)}-\mu)\,\varepsilon_{k-}^2/E_k^{(1)}\right)$$

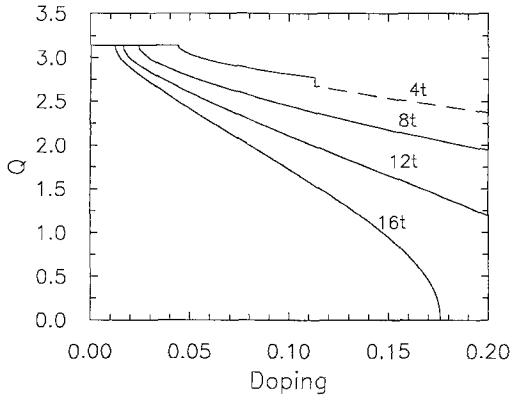

Fig. 4. Spiral wave-vector $\mathbf{Q}$ as function of doping δ for $U=4t$, $8t$, $12t$, $16t$ at $T=0.1t$. Full curve: $\mathbf{Q}=(Q,Q)$, dashed curve: $\mathbf{Q}=(Q,\pi)$

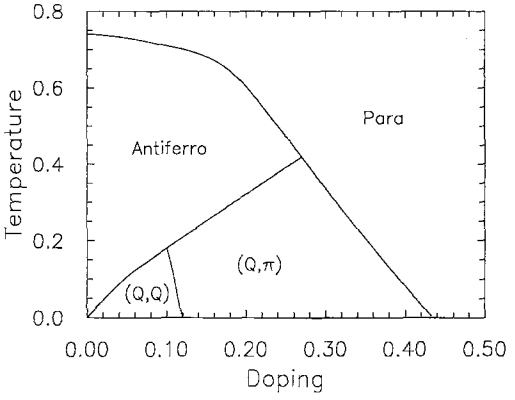

Fig. 5. $\delta-T$ phase diagram for $U=4t$. The temperature T is given in units of the hopping parameter t

where $E_k^{(1)}=-\sqrt{\varepsilon_{k-}^2+\Delta^2}$ is the dispersion of the lower antiferromagnetic band. In lowest order in t/U the doping where $\partial^2 F/\partial Q^2$ changes from positive to negative sign and the antiferromagnetic state becomes unstable is given by

$$\delta_{AF}=\frac{2T}{U}. \tag{4.2}$$

The x-component of the spiral wavevector $\mathbf{Q}$ as a function of doping at $T=0.1t$ for $U=4t$, $8t$, $12t$, $16t$ is shown in Fig. 4. The sharp drop of Q at δ_{AF} follows a squareroot law. For larger doping the differences between finite and zero temperature results are getting smaller, so that here only results for doping up to $\delta=0.2$ are presented. The $\delta-T$ phase diagram for $U=4t$ is displayed in Fig. 5. With increasing temperature the antiferromagnetic region is growing roughly linear in surprisingly good agreement with formula (4.2) which was derived for large U.

5. Summary

In summary I have investigated the phase diagram of the 2-d Hubbard model within Hartree-Fock theory restricted to spiral solutions. Similar results for zero temperature have been presented in [7] but with a different interpretation in terms of holon and doubly-occupied sites instead of spin up and down. The main effect of finite temperatures is to stabilize the antiferromagnetic state against forming a spiral upon doping. The tendency towards phase separation, which is characteristic for the zero temperature solutions at small doping turns out to be reduced with increasing temperature, especially for smaller values of U.

Even on Hartree-Fock level the present investigation is far from being exhaustive. Other candidates for magnetically ordered states that have been proposed are e.g. linear polarized spin-density waves, double spiral or canted states [10]. A much wider class of states is finally contained in an unrestricted Hartree-Fock approach, allowing for defects like e.g. vortices or domain walls [11, 12]. A systematic investigation of the phase diagram for all possible states, although requiring considerable computational efforts, could serve as first orientation and starting point for more involved approaches.

I would like to thank R. Frésard, X. Zotos and Prof. P. Wölfle for many stimulating discussions and helpful advice. I would also like to acknowledge financial support by the Bundesministerium für Forschung und Technologie No. 13N5501-1 and the Esprit No. 3041 programs.

References

1. Anderson, P.W.: Science **235**, 1196 (1987)
2. Hirsch, J.E.: Phys. Rev. B**31**, 4403 (1985)
3. Shraiman, B.I., Siggia, E.D.: Phys. Rev. Lett. **62**, 1564 (1989)
4. Schulz, H.J.: Phys. Rev. Lett. **64**, 1445 (1990)
5. Penn, D.R.: Phys. Rev. **4142**, 350 (1965)
6. Lindner, U., Schumacher, W.: Phys. Status Solidi B**155**, 263 (1989)
7. Sarker, S., Jayaprakash, C., Krishnamurthy, H.R., Wenzel, W.: Phys. Rev. B**43**, 8775 (1991)
8. John, S., Voruganti, P., Goff, W.: Phys. Rev. B**43**, 13365 (1991)
9. Frésard, R., Dzierzawa, M., Wölfle, P.: Europhys. Lett. **15**(3), 325 (1991)
10. Marder, M., Papanicolaou, N., Psaltakis, G.C.: Phys. Rev. B**41**, 6920 (1990)
11. Vergés, J.A., Louis, E., Lomdahl, P.S., Guinea, F., Bishop, A.R.: Phys. Rev. B**43**, 6099 (1991)
12. Kato, M., Machida, K., Nakanishi, H., Fujita, M.: J. Phys. Soc. Jpn. **59**, 1047 (1989)